

Cilia have high cAMP levels that are inhibited by Sonic Hedgehog-regulated calcium dynamics

Bryn S. Moore^a, Ann N. Stepanchick^a, Paul H. Tewson^b, Cassandra M. Hartle^a, Jin Zhang^c, Anne Marie Quinn^b, Thomas E. Hughes^b, and Tooraj Mirshahi^{a,1}

^aDepartment of Molecular and Functional Genomics, Weis Center for Research, Geisinger Clinic, Danville, PA 17822; ^bMontana Molecular, Bozeman, MT 59718; and ^cDepartment of Pharmacology, University of California, San Diego, La Jolla, CA 92093

Edited by Peter K. Jackson, Stanford University, Stanford, CA, and accepted by Editorial Board Member Kathryn V. Anderson September 30, 2016 (received for review February 15, 2016)

Protein kinase A (PKA) phosphorylates Gli proteins, acting as a negative regulator of the Hedgehog pathway. PKA was recently detected within the cilium, and PKA activity specifically in cilia regulates Gli processing. Using a cilia-targeted genetically encoded sensor, we found significant basal PKA activity. Using another targeted sensor, we measured basal ciliary cAMP that is fivefold higher than whole-cell cAMP. The elevated basal ciliary cAMP level is a result of adenylyl cyclase 5 and 6 activity that depends on ciliary phosphatidylinositol (3,4,5)-trisphosphate (PIP₃), not stimulatory G protein (G_{αs}), signaling. Sonic Hedgehog (SHH) reduces ciliary cAMP levels, inhibits ciliary PKA activity, and increases Gli1. Remarkably, SHH regulation of ciliary cAMP and downstream signals is not dependent on inhibitory G protein (G_{αi/o}) signaling but rather Ca²⁺ entry through a Gd³⁺-sensitive channel. Therefore, PIP₃ sustains high basal cAMP that maintains PKA activity in cilia and Gli repression. SHH activates Gli by inhibiting cAMP through a G protein-independent mechanism that requires extracellular Ca²⁺ entry.

cAMP | cilia | PKA | Hedgehog | PIP₃

PPrimary cilia are immotile organelles composed of specialized structural and signaling proteins (1). Primary cilia are essential for Hedgehog (HH) signaling, which is important during development and is misregulated in some cancers (2, 3). In HH signaling, there is a basal or Sonic Hedgehog (SHH)-off state during which cAMP-dependent protein kinase A (PKA) phosphorylates Gli proteins, which are then cleaved to the transcriptional repressor form (4). When SHH is present, or during the SHH-on state, Gli proteins are in the transcriptional activator form. PKA activity is thus critical for HH signaling, particularly in maintaining the basal SHH-off state. PKA has been thought to regulate Gli proteins at the base of the cilium (5); however, recently, the subunits of PKA have been detected in cilia (6).

G protein-coupled receptors (GPCRs) can modulate cAMP levels, which would control PKA activity, and several GPCRs are present in cilia. Smoothed, which translocates to cilia after SHH stimulation and is essential for HH signaling, is controversially classified as an inhibitory G protein (G_{αi/o})-coupled receptor (7, 8). Recently, GPR175, a G_{αi/o}-coupled receptor, was shown to localize to cilia and positively regulate HH signaling (9). GPR161 is important in left–right patterning (10) and couples to stimulatory G protein (G_{αs}) to activate adenylyl cyclase (AC) and produce cAMP (11). However, whether GPCR-mediated cAMP production occurs within cilia has not been established.

In addition to PKA being an important signaling molecule in regulating ciliary proteins, cAMP and Ca²⁺ are critical for regulating cilia length (12). Although many signaling molecules do exist in the small ciliary space, until recently they have only been measured in the whole cell. Measuring signaling molecules within cilia has remained challenging due to a paucity of effective tools. A FRET-based cAMP sensor was used to measure the inhibition of D1R signaling by GPR88 in the cilia; however, comparisons between whole-cell and ciliary levels were not made and HH signaling was not assayed (13). A more recent study used a different FRET sensor to study cAMP, but focused mainly on cAMP in

flagella (14). Three recent studies used cilia-targeted sensors to detect Ca²⁺ dynamics in cilia (15–17). Delling et al. (16) show that cilia have a high level of Ca²⁺ compared with the rest of the cell and that HH/Smoothed activation increases ciliary Ca²⁺. Long treatment of SHH agonist was required for the increased ciliary Ca²⁺, suggesting that Ca²⁺ entry is likely through recruitment of a Ca²⁺-permeable member of the Trp channel family (16, 18). Signaling molecules in cilia are believed to regulate pathways such as HH; however, only Ca²⁺ has been measured after stimulation of the HH pathway in the cilia specifically. Here we use cilia-targeted sensors for cAMP, PKA, and phosphatidylinositol (3,4,5)-trisphosphate (PIP₃) to delineate the unique mechanisms controlling basal PKA activity inside cilia and SHH inhibition of this activity.

Results

PKA Activity Is Elevated in Cilia. Until recently, PKA was thought to phosphorylate Gli proteins at the base of cilia under basal or SHH-off conditions due to PKA-C localization there (5). Several PKA subunits were recently detected within the cilium using cilia proximity labeling, and PKA-R1 α was detected within cilia using immunofluorescence (6). Additionally, by specifically inhibiting PKA activity within cilia, Mick et al. found that ciliary PKA activity is necessary for proper Gli3 protein processing (6). We targeted a PKA activity sensor, AKAR4 (19), to the cilia using the 5HT6 receptor (Fig. 1A). Measurement of basal whole-cell PKA activity using AKAR4 or cilia-targeted AKAR4 (5HT6-AKAR4) in nonciliated mouse embryonic fibroblasts (MEFs) shows similar levels of PKA activity (Fig. 1B). However, localized PKA activity within cilia is significantly higher (Fig. 1B). Because

Significance

Primary cilia are immotile organelles composed of specialized structural and signaling proteins that are essential for Hedgehog (HH) signaling. cAMP-dependent protein kinase (PKA) critically regulates HH signaling, maintaining transcriptional repression. Ciliary PKA activity is critical for HH regulation; however, the signaling steps regulating PKA activity within cilia remain unclear/unexplored. Targeted sensors were used to measure signaling molecules specifically within cilia. We found that cilia have basally high cAMP and PKA activity, controlled by phosphatidylinositol (3,4,5)-trisphosphate, not G proteins. Sonic Hedgehog stimulation reduces ciliary cAMP and PKA activity, which is dependent on Ca²⁺ dynamics.

Author contributions: B.S.M. and T.M. designed research; B.S.M., A.N.S., C.M.H., and T.M. performed research; P.H.T., J.Z., A.M.Q., and T.E.H. contributed new reagents/analytic tools; B.S.M., A.N.S., and T.M. analyzed data; and B.S.M. and T.M. wrote the paper.

Conflict of interest statement: P.H.T., A.M.Q., and T.E.H. declare competing financial interests as employees of Montana Molecular, a for-profit company.

This article is a PNAS Direct Submission. P.K.J. is a Guest Editor invited by the Editorial Board.

¹To whom correspondence should be addressed. Email: tmirshahi@geisinger.edu.

This article contains supporting information online at www.pnas.org/lookup/suppl/doi:10.1073/pnas.1602393113/-DCSupplemental.

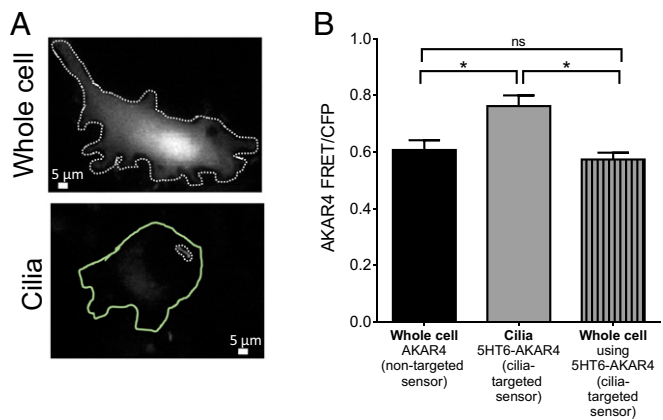


Fig. 1. (A) Images of mouse embryonic fibroblasts expressing the PKA sensor AKAR in the whole cell or cilia (5HT6-AKAR4). The dotted lines represent the regions of interest that were measured for the whole cell or cilia. The solid green line outlines the whole cell of the cell expressing the cilia-targeted PKA sensor. (B) FRET measured in cells that had not formed cilia is similar for AKAR4 and 5HT6-AKAR4, indicating that the 5HT6 tag does not alter AKAR4 response. When measured in cilia, higher FRET ratios are detected, indicating high PKA activity in cilia compared with the rest of the cell ($*P < 0.05$, compared with the whole cell; $n = 3$ experiments). ns, not significant. Data are presented as mean \pm SEM.

PKA activity is high in cilia and dependent on cAMP, we measured cAMP levels with a fluorescent sensor targeted to cilia.

Development of a Cilia-Targeted cAMP Sensor. We adapted a genetically encoded single-color intensimetric cAMP sensor, cADDis (20), for use as a cilia-targeted and ratiometric sensor. To target the sensor to the cilia, we attached cADDis to the 5HT6 receptor (Fig. 2A–C). To make the sensor ratiometric, we attached mCherry (Fig. 2A and C), whose fluorescence does not change in response to cAMP (Fig. 2D and E). The mCherry-tagged cADDis showed a similar response to direct stimulation

of AC with forskolin or L-858051, a water-soluble analog of forskolin (Fig. S14). cADDis shows progressively diminished fluorescence in response to cAMP production after application of increasing concentrations of L-858051, whereas mCherry intensity remains constant (Fig. 2D and E). Because the mCherry fluorescence does not change, we can use the mCherry/cADDis ratio to make comparisons between different regions of interest and different treatments. Changes in cAMP levels, expressed as mCherry/cADDis, in response to L-858051 are shown in Fig. 2F. Importantly, 5HT6-mCherry-cADDis and mCherry-cADDis reported similar cAMP levels in the whole cell (Fig. S1B). To address whether tagging with the 5HT6 receptor influences sensor response, we targeted mCherry-cADDis to the cilia using either Arl13b or somatostatin receptor 3 (SST3R) and measured similar mCherry/cADDis ratios (Fig. S1C). Having established that targeting the sensor to cilia does not affect sensor response, we used 5HT6-mCherry-cADDis to directly test cAMP signaling in cilia after G-protein stimulation rather than a proteomic or immunofluorescence approach. This approach affords accurate measurement of cAMP signal within the cilium in live cells and also reports cAMP dynamics in real time. We stimulated the 5HT6 receptor, a member of the stimulatory GPCR family, and measured the sensor response in cilia and found that cilia can respond to GPCR stimulation (Fig. 2G and H).

Cilia Have High Levels of cAMP. Although a FRET-based cAMP sensor targeted to cilia was previously reported, it was not used to compare cAMP levels between cilia and the whole cell (13). To accurately determine cAMP concentrations, we assayed the response of 5HT6-mCherry-cADDis expressed in MEFs to varying doses of a cell-permeant analog of cAMP, using live-cell imaging, as described previously (21). The cell-permeable analog of cAMP, 8-bromo-2'-O-methyladenosine-3',5'-cyclic monophosphate acetoxymethyl ester (8-Br-2'-O-Me-cAMP-AM), has a similar, but slightly left-shifted, dose response compared with cAMP in vitro due to accumulation within cells (21). The cell-permeable cAMP analog allows us to approximate concentrations and compare these measurements between the whole cell and cilia. We calibrated 5HT6-mCherry-cADDis in both cilia and cells that had not formed cilia (whole cell) (Fig. 3A). The dose responses from cilia

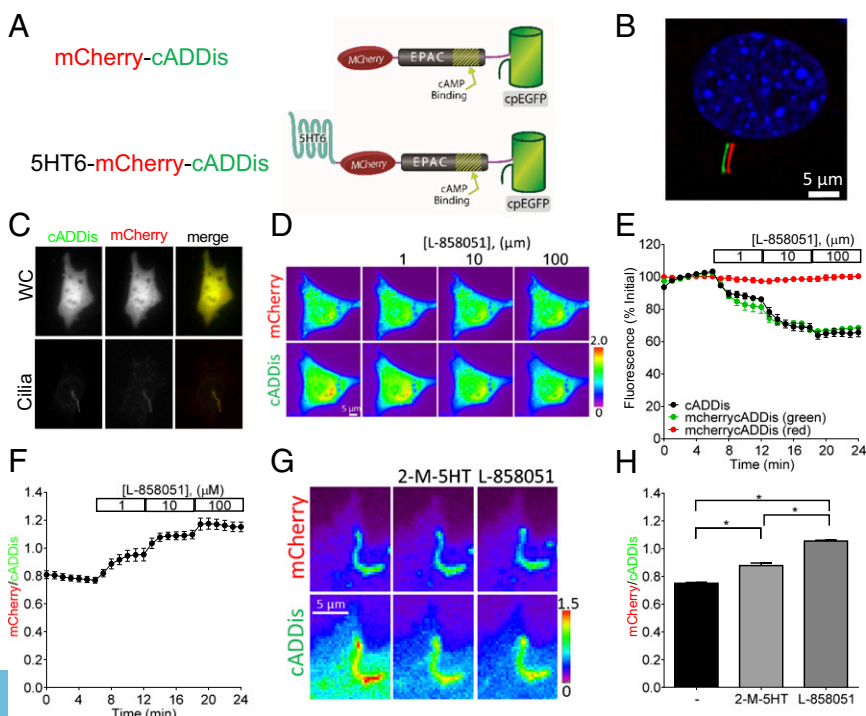


Fig. 2. (A) Cartoon depiction of mCherry-cADDis and cilia-targeted 5HT6-mCherry-cADDis. (B) Colocalization of 5HT6-mCherry-cADDis and immunostained Arl13b in MEFs that are also DAPI-stained. The red channel is pixel-shifted. (C) Green and red fluorescence from whole cells (WC) expressing mCherry-cADDis and cilia-targeted mCherry-cADDis. (D) Response of mCherry-cADDis to AC activation by 1, 10, and 100 μ M L-858051 concentrations. The red fluorescence from mCherry remains constant whereas the green fluorescence from cADDis diminishes with AC stimulation. (E) Summary fluorescence change in cADDis alone (black), mCherry in mCherry-cADDis (red), and cADDis in mCherry-cADDis (green) in response to various L-858051 concentrations. The reduction of green fluorescence in cADDis ($n = 9$ cells) and mCherry-cADDis ($n = 8$ cells) is similar. mCherry intensity does not change in response to AC stimulation. (F) Quantification of mCherry/cADDis intensity reflects relative cAMP levels ($n = 8$ cells). (G) Ciliary cADDis fluorescence diminishes in response to a 5-min stimulation of the 5HT6 receptor using 100 nM 2-methyl-5-hydroxytryptamine (2-M-5HT) as well as direct AC activation by application of 100 μ M L-858051 for 5 min. mCherry fluorescence remains constant throughout. (H) Receptor or AC-stimulated cAMP levels in cilia as described in G, measured using the mCherry/cADDis ratio, normalized to basal ciliary cAMP levels ($*P < 0.05$; $n = 7$ cilia). Data are presented as mean \pm SEM.

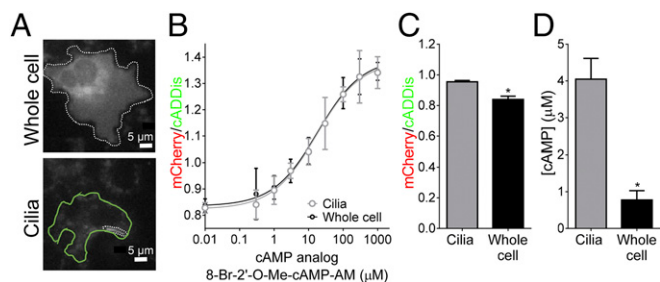


Fig. 3. (A) Images of 5HT6-mCherry-cADDIs-expressing cells with a cilium and in nonciliated cells (whole cell). The dotted lines represent the region of interest measured. The solid green line outlines the whole cell of the cell expressing the cilia-targeted 5HT6-mCherry-cADDIs. (B) Dose response to the cell-permeable cAMP analog 8-Br-2'-O-Me-cAMP-AM. Cells expressing 5HT6-mCherry-cADDIs were incubated with the cyclase inhibitor MDL-12330A to inhibit cAMP production, and then the sensor intensity was measured after addition of the cell-permeable cAMP analog ($n = 3$; 6 to 10 ROIs per point for each experiment). The mCherry/cADDIs ratios were plotted versus [cAMP analog] to produce the dose response. (C) The ratio of mCherry to cADDIs is higher in cilia compared with the whole cell, demonstrating that cilia have higher basal cAMP levels compared with the whole cell ($*P < 0.05$; $n = 3$ experiments). (D) Ciliary cAMP concentrations are five times higher than whole-cell levels, determined by interpolation of ratios on a standard curve ($*P < 0.05$; $n = 3$; 6 to 10 ROIs per experiment). Data are presented as mean \pm SEM.

and the whole cell are indistinguishable, and show that the sensor has a dynamic range that saturates in response to cAMP (Fig. 3B). Importantly, the mCherry/cADDIs ratio does vary between cell types and even different preparations of MEFs, so it is extremely important to calibrate the sensor for each cell type used (Fig. 3 and Fig. S2). Therefore, experiments comparing cilia versus the whole cell or any treatments were each completed in the same batch of cells on the same day with the same settings. Based on the dose response, 5HT6-mCherry-cADDIs is capable of reporting biologically relevant cAMP dynamics in cilia and the whole cell (300 nM to 100 μ M) (Fig. 3B).

We used 5HT6-mCherry-cADDIs to approximate cAMP concentrations in the whole cell and cilia. The average mCherry/cADDIs ratio in the whole cell was 0.84, corresponding to \sim 800 nM cAMP (Fig. 3C and D). Others have calibrated basal cAMP between \leq 100 nM and 1.2 μ M (21). In cilia, mCherry/cADDIs ratio was 0.95 corresponding to \sim 4 μ M cAMP, approximately fivefold higher than whole-cell levels (Fig. 3C and D). The dose response using 8-Br-2'-O-Me-cAMP-AM is left-shifted but parallel to the dose response using cAMP in vitro (21) and therefore the absolute concentrations in the cilia and whole cell may be slightly lower than what we estimate, but the fivefold concentration difference between the cilia and whole cell is accurate. We confirmed the multifold higher cAMP levels in cilia compared with the whole cell in a mouse kidney inner medullary collecting duct cell line (IMCD3) (Fig. S2).

Basal cAMP Levels Are Due to PIP₃. To elucidate differences in ciliary cAMP dynamics from the whole cell, we inhibited cAMP production with the broad-spectrum cyclase inhibitor MDL-12330A and prevented cAMP breakdown by phosphodiesterases (PDEs) with IBMX. MDL-12330A reduces cAMP in the cilia but not the whole cell (Fig. 4A). Furthermore, IBMX increases ciliary but not whole-cell cAMP (Fig. 4B). Given the precise spatiotemporal regulation of cAMP in cytosol (22), it is not surprising that inhibition of cyclase or PDE did not alter basal cAMP levels. Together, these data show tonic production of cAMP in cilia but not the whole cell in a cyclase-dependent manner.

Adenylyl cyclase 5 and 6 (AC5/6) localize to cilia (23). We performed siRNA knockdown in IMCD3 cells to test whether the tonic cAMP production depends on AC5/6. We detect both AC5 and AC6 in IMCD3 cells, with AC6 being the predominant subtype (Fig. S3). We used siRNA to both AC5 and AC6 and

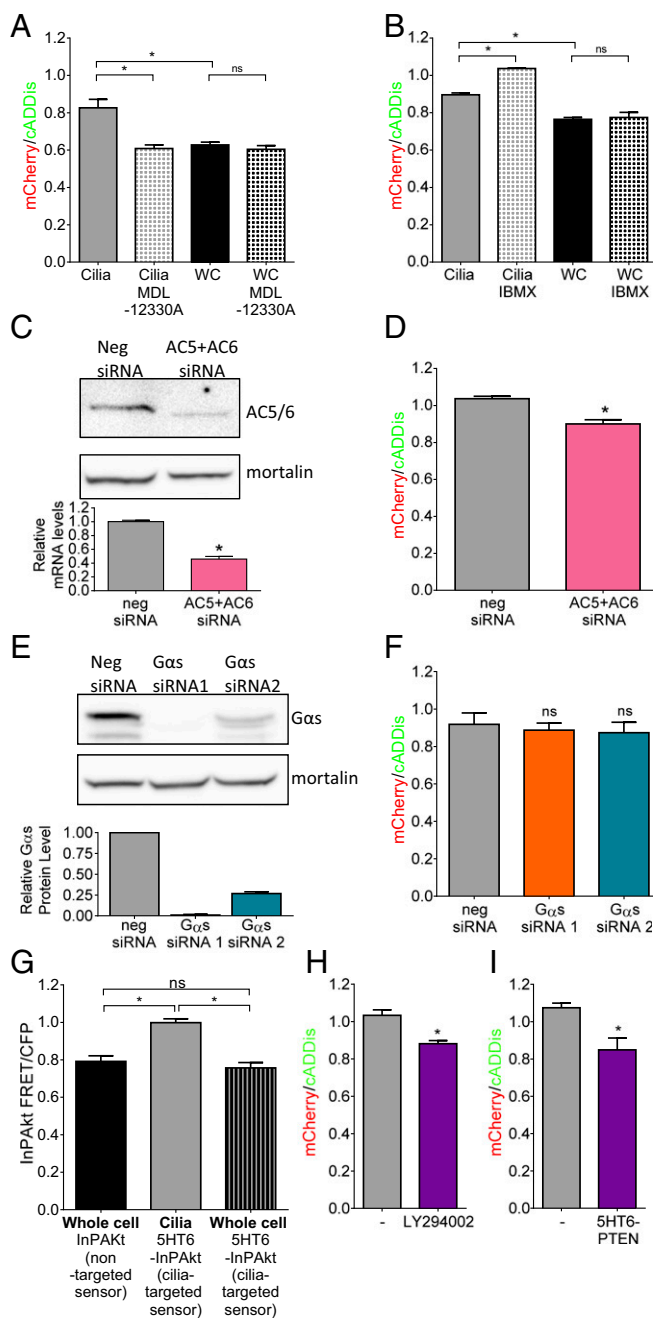


Fig. 4. (A) Direct inhibition of AC using 100 μ M MDL-12330A for 30 min reduces ciliary cAMP to whole-cell levels ($*P < 0.05$; $n = 3$ experiments) but does not affect whole-cell cAMP levels. (B) Inhibition of PDE using 100 μ M IBMX overnight increases ciliary cAMP but not whole-cell cAMP levels ($*P < 0.05$; $n = 3$ experiments). (C) Western blot using an anti-AC5/6 antibody showing effective knockdown using siRNA to AC5 and AC6; mortalin is used as a loading control. The bar graph shows relative reduction in AC6 mRNA ($*P < 0.05$). (D) Knockdown of AC5/6-reduced ciliary cAMP measured using the mCherry/cADDIs ratio ($*P < 0.05$; $n = 3$ experiments; 15 to 40 ROIs per experiment). (E) Western blot showing effective siRNA knockdown of G α_s in MEFs; mortalin is used as a loading control. The bar graph is a quantitation of three independent knockdown experiments. (F) Knockdown of G α_s does not reduce ciliary cAMP measured using the mCherry/cADDIs ratio ($n = 3$ experiments; 7 to 14 ROIs per experiment). (G) Summary FRET/CFP data from cells expressing the PIP₃ sensor InPAKT or 5HT6-InPAKT in cilia ($*P < 0.05$; $n = 3$ experiments) or the whole cell ($n = 3$ experiments) show that cilia have higher PIP₃ levels. (H) Inhibition of PI3K using 10 nM LY294002 overnight reduces basal cilia cAMP levels ($*P < 0.05$; $n = 3$ experiments). (I) Expression of the lipid phosphatase PTEN in cilia reduces cAMP levels ($*P < 0.05$; $n = 3$ experiments). Data are presented as mean \pm SEM.

achieved knockdown detected using both quantitative (q)PCR and immunoblotting (Fig. 4C). Using 5HT6-mCherry-cADDIs, we found significant reduction of basal ciliary cAMP in cells where AC5/6 are knocked down (Fig. 4D), indicating that AC5/6 are responsible for tonic ciliary cAMP production. To test whether putative basal GPCR activity through G_{α_s} is responsible for the constitutive AC activity and high basal cAMP levels, we used siRNA to knock down G_{α_s} in MEFs. We knocked down G_{α_s} using two different siRNAs (99% and 74% knockdown, respectively) (Fig. 4E). Knockdown by either siRNA results in complete inhibition of cAMP signaling in cilia after stimulation by β_2 AR, indicating effective functional knockdown of G_{α_s} (Fig. S4A). Knockdown of G_{α_s} , however, does not affect basal ciliary cAMP levels (Fig. 4F), suggesting a G protein-independent AC5/6 regulation of tonic cAMP production.

PIP₃ is capable of regulating AC5/6 activity (24), so we hypothesized that this noncanonical pathway for AC5/6 activation may play a role in cAMP dynamics in cilia. We therefore determined relative PIP₃ levels in the whole cell compared with cilia by targeting the FRET-based PIP₃ sensor InPAkt (25) to cilia by attaching the 5HT6 receptor. Live-cell imaging shows significantly higher PIP₃ levels in cilia compared with the whole cell (Fig. 4G). Phosphatidylinositol 3-kinase (PI3K) phosphorylates PI(4,5)P₂ to produce PI(3,4,5)P₃ (26). Inhibition of PI3K using LY294002 significantly reduces ciliary cAMP levels (Fig. 4H), suggesting that PIP₃ is required for cAMP production in cilia. To reduce PIP₃ levels specifically in cilia of MEFs, we used a nonpharmacological approach by targeting PTEN to cilia with 5HT6. PTEN is a 3' phosphatase that dephosphorylates PI(3,4,5)P₃ to produce PI(4,5)P₂ with 200-fold more effectiveness for PIP₃ than other phosphoinositides (27). By attaching 5HT6 to PTEN, we can localize its phosphatase activity to the cilia. Expression of 5HT6-PTEN reduces ciliary cAMP levels to those found in the whole cell (Fig. 4I). By preventing PIP₃ formation (Fig. 4H) or increasing PIP₃ breakdown (Fig. 4I), we show that basally high ciliary cAMP is due to G protein-independent AC5/6 activity mediated by PIP₃.

SHH Increases Ca²⁺ and Reduces cAMP and PKA. AC5 and AC6 are inhibited by Ca²⁺ (28). The Smoothed agonist SAG raises [Ca²⁺] in cilia (16) and increases Ca²⁺ current in cilia through Trp channels that are inhibited by Gd³⁺ (17). We used the cilia-targeted Ca²⁺ sensor 5HT6-mCherry-GECO1.0 (15) to measure Ca²⁺ levels in response to SHH. Ciliary Ca²⁺ levels increase upon SHH stimulation and are inhibited by Gd³⁺ (Fig. 5A). Because SHH increases ciliary Ca²⁺ and the ciliary AC5 and AC6 are inhibited by Ca²⁺ (28), we determined the effect of SHH on ciliary cAMP. Treatment of MEFs with SHH and other Smoothed activators reduces ciliary cAMP (Fig. 5B and Fig. S5). SHH also prevents GPCR-mediated and direct AC-activated production of cAMP (Fig. S4B). Gd³⁺, which blocks Ca²⁺ entry, inhibits the SHH-mediated reduction in cAMP (Fig. 5B and Figs. S4B and S5A). Ruthenium red, another channel blocker, also inhibits the SHH-mediated cAMP reduction (Fig. S5B). Although there is very little cAMP basally in the whole cell (Fig. 3C and D), SHH does not detectably affect the cAMP in the whole cell. Our data suggest that inhibition of AC5 and AC6 by Ca²⁺ is the mechanism of SHH reduction of cAMP in cilia. The identity of I_{cilia}, the calcium-permeable ciliary current, remains controversial (17, 29). We detect significant levels of PKD2 but not PKD2L1 transcripts in IMCD3 cells and MEFs (Fig. S6). These data suggest that PKD2 is the likely channel-mediating Ca²⁺ effect that we report here; however, the identity of I_{cilia} in each cell type needs further study and empirical determination.

Mick et al. have shown that SAG-mediated reduction of the Gli3 repressor is dependent on ciliary PKA activity (6). Although it has been speculated that stimulation of the HH pathway leads to decreased PKA activity, this link has not been tested within cilia. The high basal cAMP in cilia that we measured (Fig. 3C and D) is sufficient to activate PKA (30), and indeed there is higher PKA activity in cilia compared with the whole cell (Fig. 1B). Using

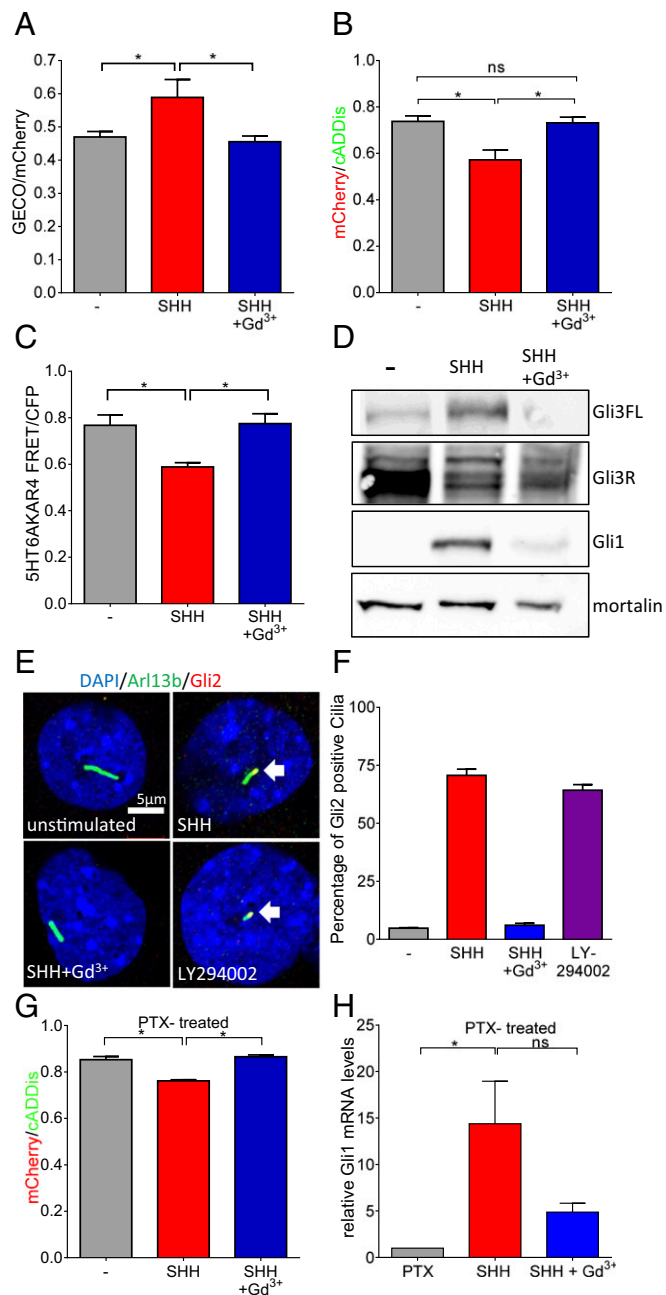


Fig. 5. SHH effects on Ca²⁺, cAMP, PKA, and Gli. (A) Overnight application of 100 μ M Gd³⁺ inhibits SHH (10 nM)-mediated increase in ciliary Ca²⁺ ($*P < 0.05$; $n = 3$ experiments; 7 to 12 ROIs each). (B) SHH reduces ciliary cAMP; Gd³⁺ prevents the effect of SHH ($*P < 0.05$; $n = 3$ experiments). (C) SHH inhibits PKA activity in cilia measured using the PKA sensor AKAR4. Gd³⁺ prevents SHH inhibition of PKA ($*P < 0.05$; $n = 3$ experiments). (D) In MEFs, SHH reduces Gli3R and increases Gli3-FL and Gli1; Gd³⁺ inhibits SHH effects. Western blot is representative of three similar experiments. Mortalin is used as a loading control. (E) Immunofluorescence to detect localization of transfected Gli2-HA in cilia after various treatments. Arl13b immunofluorescence (green) is used to demarcate cilia; nuclei are stained using DAPI. Gli2 localizes to cilia after SHH treatment. The SHH effect on Gli2 localization is inhibited by Gd³⁺. Inhibition of PI3K leads to localization of Gli2 to cilia in the absence of SHH. White arrows indicate colocalization. (F) Summary data for ciliary localization of Gli2-HA after various treatments. The data are from two independent experiments. A total of 42 to 55 cilia were counted for the four conditions to determine the percentages. (G) In MEFs treated with PTX (250 ng/mL; overnight), SHH maintains its ability to reduce ciliary cAMP whereas Gd³⁺ still prevents the SHH effect ($*P < 0.05$; $n = 3$ experiments). (H) SHH increase of Gli1 expression is also maintained after PTX treatment but was prevented by Gd³⁺ ($*P < 0.05$). Data are presented as mean \pm SEM.

the cilia-targeted AKAR4, we found that SHH treatment results in reduced PKA activity in cilia that is prevented by cotreatment with Gd^{3+} (Fig. 5C). To determine regulation of downstream signaling to Gli proteins by SHH and Ca^{2+} , we measured Gli3 and Gli1 proteins after treatment with SHH with or without blocking Ca^{2+} entry with Gd^{3+} . Fig. 5D shows effects of SHH on Gli3R, Gli3-FL, and Gli1 that were all prevented by Gd^{3+} . Using immunofluorescence to detect an HA-tagged Gli2, we also show that SHH stimulation leads to Gli2 localization to cilia that is prevented by Gd^{3+} (Fig. 5E). Additionally, inhibition of PI3K leads to Gli2 localization to cilia (Fig. 5E), which further supports a role for PIP_3 -mediated regulation of cAMP signaling. Summary data for Gli2 localization after different treatments are shown in Fig. 5F.

Having demonstrated the importance of Ca^{2+} in SHH-mediated signaling through cAMP and PKA, we next addressed the potential of Smoothed signaling through $G\alpha_{i/o}$ to inhibit ACs, resulting in the reduction of cAMP. Pertussis toxin (PTX) treatment effectively inhibits $G\alpha_{i/o}$ activity in cilia (Fig. S4C). Remarkably, in the presence of PTX, SHH still reduces cAMP but the cAMP reduction can be prevented by Gd^{3+} (Fig. 5G). Furthermore, PTX did not prevent the increase in Gli1 expression after HH signaling, whereas Gd^{3+} effectively inhibited this effect (Fig. 5H). Therefore, SHH regulation of ciliary cAMP is not dependent on $G\alpha_{i/o}$ signaling but rather Ca^{2+} entry through a Gd^{3+} -inhibited channel.

Discussion

By directly measuring cAMP in cilia, we have established that the basal concentration of cAMP in cilia is not only higher than in the whole cell but also high enough to sustain PKA activity (30). Primary cilia of MEFs are capable of responding to signals from stimulatory GPCRs (Fig. 2G and H); however, the basally high cAMP level in cilia depends on adenylyl cyclase 5/6 activity that requires PIP_3 but not stimulatory G proteins. Others have reported that $PI(4,5)P_2$ and INPP5E play critical roles in ciliary signaling (31) and that inhibition of PI3K prevents IGF-I-stimulated Akt and SHH-mediated increase in Gli activity in a luciferase assay (32). Additionally, cross-talk between inhibition of HH and PI3K expression was also reported in some medulloblastomas (33). However, those previous reports did not establish a specific role for PIP_3 in ciliary signaling. We show that AC5/6 are key players in regulating ciliary cAMP. Given the recent finding that PIP_3 regulates AC5/6 (24), we used selective pharmacological (27) and genetic overexpression strategies to reduce PIP_3 and effectively reduce ciliary cAMP levels. We therefore conclude that PIP_3 is the key player in regulating AC5/6 and maintaining high cAMP levels in cilia.

Previous reports have suggested a role for HH-regulated Ca^{2+} signaling during development (34) and in metabolic regulation (35). We show that HH signaling controls Ca^{2+} dynamics to regulate ciliary cyclases and downstream signaling through cAMP to PKA and Gli proteins (Fig. 6). Our data do not eliminate the role for G-protein pathways in regulating specific ciliary signaling, such as those shown for GPCRs (36, 37). Likewise, we recognize that specific cell types or certain developmental time points may require additional regulation of cAMP by stimulatory or inhibitory GPCRs to regulate HH signaling (38).

The identity of the channel responsible for Ca^{2+} entry in cilia is a matter of current debate (17, 29). In the two cell lines that we use, PKD2 but not PKD2L1 was detected using RT-PCR and qPCR. However, different cells from other tissues may use other channels to accumulate Ca^{2+} in the cilium (39). Regardless of which channel mediates the Ca^{2+} current, we show cAMP, PKA, and Gli protein regulation by this Gd^{3+} -sensitive Ca^{2+} entry. Delling et al. report that SAG stimulation does not immediately affect Ca^{2+} levels in cilia but that after 24 h Ca^{2+} levels are increased (16), and suggest that the rise in Ca^{2+} is due to the recruitment of calcium-permeable Trp channels. Although short-term effects on Gli proteins of SHH stimulation have been seen (40), the full effects are not seen until much later (at least 16 h after SHH stimulation). Undetected changes in cAMP dynamics

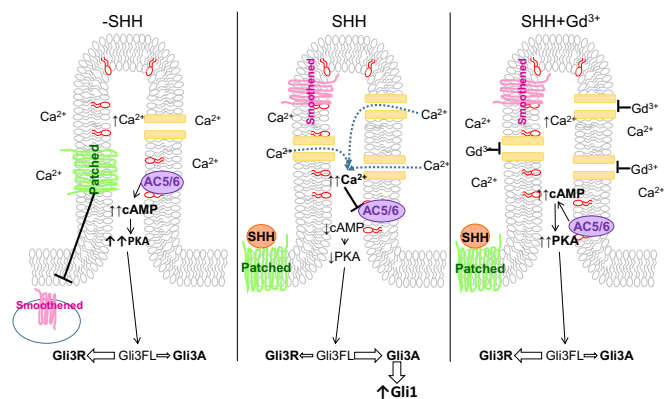


Fig. 6. Model of ciliary HH signaling. (Left) Under basal conditions, PIP_3 (depicted in red on the inner leaflet of the membrane) maintains AC5/6 activity in the cilia, resulting in high cAMP concentration. Relative to the whole cell, high Ca^{2+} is present in the cilia. Basal cAMP activates PKA, shifting the Gli balance in favor of GliR. (Middle) After SHH stimulation, Smoothed translocates to the ciliary membrane, and channel activity and Ca^{2+} levels are increased (12) that inhibit AC5/6. The resulting reduction in cAMP reduces PKA activity, shifting the balance to GliA. (Right) Gadolinium blocks Ca^{2+} entry through channels, inhibiting the effects of SHH.

or an undetermined mechanism may regulate the fast response of Gli proteins. However, to see the full effect of SHH stimulation, prolonged stimulation is required.

By measuring signaling molecules in cilia, we find that Ca^{2+} and phospholipids regulate cAMP signaling in cilia, obviating the need for G-protein signaling. As is the case for Ca^{2+} concentration in cilia, production of a small number of cAMP molecules significantly increases cAMP concentration within the small ciliary space. Nevertheless, those few cAMP molecules are sufficient to sustain PKA activity in the cilia and maintain GliR. Our data highlight the unique environment that exists within cilia, in which local PIP_3 levels cause basally high cAMP and PKA levels and maintain Gli proteins in the repressor form. Finally, SHH increase in Ca^{2+} and reduction of ciliary cAMP are sufficient to reduce PKA activity and change Gli processing.

Experimental Procedures

Refer to *SI Experimental Procedures* for full methods.

Molecular Biology. 5HT6-mCherry-G-GECO1.0 (15), PTEN-GFP, Arl13b-GFP, and pCEFL 3x-HA-Gli2 were obtained from Addgene. Somatostatin receptor 3 was purchased from the DNA Resource Center. The cADDis sensor was developed by Montana Molecular (montanamolecular.com). The PKA sensor AKAR4 (19) and PIP_3 sensor InPAKT (25) have been described elsewhere. All sensors were targeted to the cilia by the 5HT6 receptor or 5HT6-mCherry. mCherry was subcloned in-frame to the 5' end of cADDis to create mCherry-cADDis. Arl13b and SST3R were cloned in-frame to the N terminus of mCherry-cADDis.

Cell Culture of MEFs and IMCD3. Mouse embryonic fibroblasts were isolated from embryonic day (E)13.5 embryos as described (41), and experiments were carried out within four passages. MEFs or mouse IMCD3 cells were nucleofected using the Neon Transfection System (Life Technologies) and serum-starved 16 to 22 h before imaging to induce ciliogenesis.

Imaging. Cells were rinsed twice with imaging low K-buffer containing 25 mM Hepes, 114 mM NaCl, 2.2 mM KCl, 2 mM $CaCl_2$, 2 mM $MgCl_2$, 22 mM $NaHCO_3$, 1.1 mM NaH_2PO_4 , and 2 mM glucose (pH 7.4). Live cells were imaged on an inverted Olympus spinning-disk confocal microscope with MetaMorph image-acquisition software (Molecular Devices) and processed with ImageJ (NIH).

cAMP Quantitation. Responses of the 5HT6-mCherry-cADDis sensor to varying doses of cAMP were measured following the protocol of Börner and colleagues (21). cAMP levels of MDL-12330A-treated cells were collected followed by exposure to 0.01 to 100 μ M cell-permeable cAMP analog 8-Br-2'-O-Me-cAMP-AM

(Axxora), which was shown to have the same affinity for EPAC2 as cAMP (21). The mCherry/cADDi sensor ratios were calculated and the dose response was fitted with a four-parameter curve using Prism 6 (GraphPad Software). mCherry/cADDi ratios were input as unknown Y values in Prism and, using the four-parameter curve fit, x values were interpolated to calculate the cAMP concentration in cilia or the whole cell.

Image Processing. For each experiment a specific region of interest (ROI) was selected: Whole-cell imaging data from the entire cell were captured, ciliary signaling-targeted sensors were used that localized primarily to cilia, and then ROIs were selected to include only cilia and exclude any extraneous sensor in the rest of the cell.

Expression of Cilia-Targeted PTEN. 5HT6-PTEN (described above) was cotransfected into MEFs with 5HT6-mCherry-cADDi. Cells were serum-starved overnight and imaged the following day as described above.

Gli Western Blot. MEFs were serum-starved and treated for 16 h overnight with 10 nM Sonic Hedgehog and/or 25 μ M gadolinium in DMEM + 0.2% BSA. Protein lysates were run on a 7.5% Tris-HCl gel and transferred to nitrocellulose membranes. The membrane was probed overnight at 4 °C with Gli3 antibody (R&D Systems) diluted 1:1,000. The secondary antibody used was donkey anti-goat HRP at 1:20,000 (Jackson ImmunoResearch). Stripped membranes were probed overnight with Gli1 antibody at 1:1,000 (Cell Signaling Technology) or mortalin at 1:1,000 (Antibodies Incorporated). Secondary antibodies used were donkey anti-rabbit HRP at 1:3,000 (for Gli1) and goat anti-mouse HRP at 1:3,000 (for mortalin).

Knockdowns, Western Blots, and cAMP Levels. MEFs were transfected with negative control (SI03650318), GNAS (SI01053983 and SI01053990), or AC5

and AC6 (SI00890106 and SI02685753) siRNAs using the Neon Transfection System (Life Technologies). Cells were serum-starved overnight before analysis. Forty-eight hours after siRNA and 5HT6-mCherry-cADDi nucleofection, cilia were imaged and protein and/or RNA were harvested. For Western blotting, the membrane was probed using anti-G α_x antibody (GeneTex) at 1:1,000 or anti-AC5/6 antibody (Santa Cruz; SC-590) at 1:200 overnight at 4 °C and donkey anti-rabbit HRP or donkey anti-rabbit HRP secondary antibodies. Blots were stripped and probed for mortalin as a loading control as described above. qPCR was performed using TaqMan Gene Expression Assays (Applied Biosystems) for mouse Adcy5 (Mm00674122_ml), Adcy6 (Mm00475772_ml), and GAPDH (Mm99999915_gl).

Pertussis Toxin Inhibition of G $\alpha_{i/o}$. 5HT6-mCherry-cADDi transfected cells were serum-starved and treated with SHH (10 nM) \pm Gd $^{3+}$ (100 μ M) and PTX (250 ng/mL) for 18 to 22 h. The cAMP levels of cells treated with boiled (inactivated) PTX (250 ng/mL) were not different from untreated controls.

ACKNOWLEDGMENTS. The authors thank Anne Moon (Geisinger Clinic) and Norann Zaghoul (University of Maryland) for their critical review and comments on the manuscript; Jonathan Luo and Thomas Hynes for developing the original ImageJ scripts used for image analysis; and Rose Quinn for creating the artwork in Fig. 1. We also thank the following for depositing plasmids with Addgene that were used in this study: T. Inoue for 5HT6-mCherry-G-GECO1.0, A. Ross for PTEN-GFP, P. Beachy for HA-Gli2, and T. Casparly for L13-Arl13b-GFP. This work was supported by funds from the Geisinger Clinic, Pennsylvania CURE Formula Grant 4100068713, and NIH R01GM111913 (to T.M.), National Science Foundation IIP-1430878 (to A.M.Q.), NIH R44NS082222 (to A.M.Q. and T.E.H.), Montana STTR/SBIR Matching Funds Program 13-50-RCSBIR-003 Small Business Innovation Research Match Award from the Montana Department of Commerce (to A.M.Q.), and NIH R01 DK073368 and R01 GM111665 (to J.Z.).

- Berbari NF, O'Connor AK, Haycraft CJ, Yoder BK (2009) The primary cilium as a complex signaling center. *Curr Biol* 19(13):R526–R535.
- Pasca di Magliano M, Hebrok M (2003) Hedgehog signalling in cancer formation and maintenance. *Nat Rev Cancer* 3(12):903–911.
- Yang L, Xie G, Fan Q, Xie J (2010) Activation of the hedgehog-signaling pathway in human cancer and the clinical implications. *Oncogene* 29(4):469–481.
- Wang B, Fallon JF, Beachy PA (2000) Hedgehog-regulated processing of Gli3 produces an anterior/posterior repressor gradient in the developing vertebrate limb. *Cell* 100(4):423–434.
- Tuson M, He M, Anderson KV (2011) Protein kinase A acts at the basal body of the primary cilium to prevent Gli2 activation and ventralization of the mouse neural tube. *Development* 138(22):4921–4930.
- Mick DU, et al. (2015) Proteomics of primary cilia by proximity labeling. *Dev Cell* 35(4):497–512.
- Riobo NA, Saucy B, Dilizio C, Manning DR (2006) Activation of heterotrimeric G proteins by Smoothened. *Proc Natl Acad Sci USA* 103(33):12607–12612.
- Philipp M, Caron MG (2009) Hedgehog signaling: Is Smo a G protein-coupled receptor? *Curr Biol* 19(3):R125–R127.
- Singh J, Wen X, Scales SJ (2015) The orphan G protein-coupled receptor Gpr175 (Tpra40) enhances Hedgehog signaling by modulating cAMP levels. *J Biol Chem* 290(49):29663–29675.
- Leung T, et al. (2008) The orphan G protein-coupled receptor 161 is required for left-right patterning. *Dev Biol* 323(1):31–40.
- Mukhopadhyay S, et al. (2013) The ciliary G-protein-coupled receptor Gpr161 negatively regulates the Sonic hedgehog pathway via cAMP signaling. *Cell* 152(1–2):210–223.
- Besschetnova TY, et al. (2010) Identification of signaling pathways regulating primary cilium length and flow-mediated adaptation. *Curr Biol* 20(2):182–187.
- Marley A, Choy RW, von Zastrow M (2013) GPR88 reveals a discrete function of primary cilia as selective insulators of GPCR cross-talk. *PLoS One* 8(8):e70857.
- Mukherjee S, et al. (2016) A novel biosensor to study cAMP dynamics in cilia and flagella. *eLife* 5:e14052.
- Su S, et al. (2013) Genetically encoded calcium indicator illuminates calcium dynamics in primary cilia. *Nat Methods* 10(11):1105–1107.
- Delling M, DeCaen PG, Doerner JF, Febvay S, Clapham DE (2013) Primary cilia are specialized calcium signalling organelles. *Nature* 504(7479):311–314.
- DeCaen PG, Delling M, Vien TN, Clapham DE (2013) Direct recording and molecular identification of the calcium channel of primary cilia. *Nature* 504(7479):315–318.
- Semmo M, Kottgen M, Hofferr A (2014) The TRPP subfamily and polycystin-1 proteins. *Handb Exp Pharmacol* 212:675–711.
- Depry C, Zhang J (2011) Using FRET-based reporters to visualize subcellular dynamics of protein kinase A activity. *Methods Mol Biol* 756:285–294.
- Tewson PH, Martinka S, Shaner NC, Hughes TE, Quinn AM (2016) New DAG and cAMP sensors optimized for live-cell assays in automated laboratories. *J Biomol Screen* 21(3):298–305.
- Börner S, et al. (2011) FRET measurements of intracellular cAMP concentrations and cAMP analog permeability in intact cells. *Nat Protoc* 6(4):427–438.
- Karpen JW, Rich TC (2004) Resolution of cAMP signals in three-dimensional microdomains using novel, real-time sensors. *Proc West Pharmacol Soc* 47:1–5.
- Vuolo L, Herrera A, Torroba B, Menendez A, Pons S (2015) Ciliary adenylyl cyclases control the Hedgehog pathway. *J Cell Sci* 128(15):2928–2937.
- Reddy GR, et al. (2015) Adenylyl cyclases 5 and 6 underlie PIP3-dependent regulation. *FASEB J* 29(8):3458–3471.
- Ananthanarayanan B, Ni Q, Zhang J (2005) Signal propagation from membrane messengers to nuclear effectors revealed by reporters of phosphoinositide dynamics and Akt activity. *Proc Natl Acad Sci USA* 102(42):15081–15086.
- Balla T (2013) Phosphoinositides: Tiny lipids with giant impact on cell regulation. *Physiol Rev* 93(3):1019–1137.
- McConnachie G, Pass I, Walker SM, Downes CP (2003) Interfacial kinetic analysis of the tumour suppressor phosphatase, PTEN: Evidence for activation by anionic phospholipids. *Biochem J* 371(Pt 3):947–955.
- Cooper DM, Karpen JW, Fagan KA, Mons NE (1998) Ca(2+)-sensitive adenylyl cyclases. *Adv Second Messenger Phosphoprotein Res* 32:23–51.
- Nauli SM, et al. (2003) Polycystins 1 and 2 mediate mechanosensation in the primary cilium of kidney cells. *Nat Genet* 33(2):129–137.
- Zhang P, et al. (2012) Structure and allostery of the PKA RII β tetrameric holoenzyme. *Science* 335(6069):712–716.
- Chávez M, et al. (2015) Modulation of ciliary phosphoinositide content regulates trafficking and Sonic Hedgehog signaling output. *Dev Cell* 34(3):338–350.
- Riobo NA, Lu K, Ai X, Haines GM, Emerson CP, Jr (2006) Phosphoinositide 3-kinase and Akt are essential for Sonic Hedgehog signaling. *Proc Natl Acad Sci USA* 103(12):4505–4510.
- Buonamici S, et al. (2010) Interfering with resistance to Smoothened antagonists by inhibition of the PI3K pathway in medulloblastoma. *Sci Transl Med* 2(51):51ra70.
- Belgacem YH, Borodinsky LN (2011) Sonic hedgehog signaling is decoded by calcium spike activity in the developing spinal cord. *Proc Natl Acad Sci USA* 108(11):4482–4487.
- Teperino R, et al. (2012) Hedgehog partial agonism drives Warburg-like metabolism in muscle and brown fat. *Cell* 151(2):414–426.
- Briscoe J, Théron PP (2013) The mechanisms of Hedgehog signalling and its roles in development and disease. *Nat Rev Mol Cell Biol* 14(7):416–429.
- Mukhopadhyay S, Rohatgi R (2014) G-protein-coupled receptors, Hedgehog signaling and primary cilia. *Semin Cell Dev Biol* 33:63–72.
- Regard JB, et al. (2013) Activation of Hedgehog signaling by loss of GNAS causes heterotopic ossification. *Nat Med* 19(11):1505–1512.
- DeCaen PG, Liu X, Abiria S, Clapham DE (2016) Atypical calcium regulation of the PKD2-L1 polycystin ion channel. *eLife* 5:e13413.
- Wen X, et al. (2010) Kinetics of hedgehog-dependent full-length Gli3 accumulation in primary cilia and subsequent degradation. *Mol Cell Biol* 30(8):1910–1922.
- Kumar P P, et al. (2014) Coordinated control of senescence by lncRNA and a novel T-box3 co-repressor complex. *eLife* 3:e02805.